REVIEW

National Science Review
4: 426–436, 2017
doi: 10.1093/nsr/nwx030
Advance access publication 15 March 2017

CHEMISTRY

Special Topic: Organic Chemistry Booming in China

Supramolecular organic frameworks (SOFs): homogeneous regular 2D and 3D pores in water

Jia Tian[1], Hui Wang[1], Dan-Wei Zhang[1], Yi Liu[2,*] and Zhan-Ting Li[1,*]

ABSTRACT

Studies on periodic porosity and related properties and functions have been limited to insoluble solid-state materials. Self-assembly provides a straightforward and efficient strategy for the construction of soluble periodic porous supramolecular organic frameworks (SOFs) in water from rationally designed molecular building blocks. From rigid tri- and tetra-armed building blocks and cucurbitu[8]ril (CB[8]), a number of two-dimensional (2D) honeycomb, square and rhombic SOFs can be generated, which is driven by CB[8]-encapsulation-enhanced dimerization of two aromatic units on the periphery of the multi-armed molecules. By utilizing the same three-component host–guest motif as the driving force, three-dimensional (3D) diamondoid and cubic SOFs can be obtained from tetrahedral and $[Ru(bipy)_3]^{2+}$-derived octahedral monomers and CB[8]. All of the 2D and 3D periodic frameworks are soluble in water, and are able to maintain the periodicity as well as the pore sizes in the solid state. 3D SOFs are highly efficient homogeneous polycationic frameworks for reversible adsorption of anionic species including organic dyes, peptides, nucleic acids, drugs, dendrimers and Wells-Dawson-typed polyoxametallates (WD-POMs). WD-POM molecules adsorbed in the $[Ru(bipy)_3]^{2+}$-based SOF can catalyse the reduction of proton to H_2 upon visible-light sensitization of $[Ru(bipy)_3]^{2+}$, which allows multiple electron transfer from $[Ru(bipy)_3]^{2+}$ to WD-POM. This review summarizes the design, formation and characterization of this new family of self-assembled frameworks, highlights their applications as homogeneous porous materials and finally outlines some future research directions.

Keywords: supramolecular organic framework, porosity, regularity, supramolecular polymer, adsorption

[1]Department of Chemistry, Collaborative Innovation Centre of Chemistry for Energy Materials (iChEM), Fudan University, Shanghai 200433, China and [2]The Molecular Foundry, Lawrence Berkeley National Laboratory, Berkeley, CA 94720, USA

***Corresponding authors.** E-mails: ztli@fudan.edu.cn; yliu@lbl.gov

Received 5 December 2016; **Revised** 15 February 2017; **Accepted** 28 February 2017

INTRODUCTION

Porous structures are important in many research fields of chemical science, such as molecular recognition, sensing, transport, separation and catalysis. Zeolite has been studied for more than 100 years, and still remains an active research target for both fundamental and practical purposes. In nature, protein channels for transmembrane transport of ions and molecules are the basis for metabolism in life. Molecular porosity is structurally very diverse. The simplest form of porosity is a unimolecular macrocycle which can produce a cavity. Macrocycles and molecules with related topologies play central roles in molecular recognition because they can realize high selectivity and stability through multivalency and cooperativity. Pioneering work on the molecular-recognition properties of crown ethers, cryptands and spherands were carried out by Pedersen, Lehn and Cram, respectively, who had been awarded Nobel Prize in Chemistry in 1987 [1–3].

The cavity of a simple macrocycle can be expanded in different ways. In a minimal three-dimensional (3D) space, it can grow into a cage as a single molecule prepared by step-by-step approaches or one-pot synthesis using the strategy of dynamic covalent chemistry [4–7], which may be dynamically open or closed to the outside environment for guest encapsulation and exchange. A cage can also be obtained through the self-assembly of two or more molecular components driven by discrete non-covalent forces [8,9]. Both kinds of cage systems may be regarded as a family of zero dimensional (0D) materials that have found wide

applications, such as in molecular recognition, reaction promotion and catalysis, and entrapment of reactive intermediates and radioactive isotopes. In particular, studies on self-assembled cages or capsules have become a very active area of supramolecular chemistry as a result of addressing challenges in creating unprecedented structural complexity for exploitation of new physical and chemical phenomena [10–12]. An aligned macrocyclic cavity in an one-dimensional (1D) space can produce a tubular structure. One prominent kind of example is carbon nanotubes, which, over the years, have been vigorously investigated for nearly all subfields of materials sciences. However, self-assembly has been demonstrated to provide the most useful approach to build diverse 1D tubular structures. One early example involves the face-to-face aggregation of cyclic peptides in the 1D direction in membranes, which is driven by intermolecular hydrogen bonding and hydrophobicity [13,14]. Recently, more rigid aromatic urea and phenylethynyl macrocycles have also found applications for generating stable supramolecular hollow tubes that can be used as microreactors [15,16]. Hollow tubular structures can also be formed by holding linear molecules into bundles through zipper-styled molecular binding [17] and helical polymers can form single-polymer tubes [18,19].

When a macrocycle 'grows' repeatedly within a plane, two-dimensional (2D) networks can be formed. Currently, two major kinds of covalently bonded 2D networks have been synthetically available: covalent organic frameworks (COFs) [20–22] and 2D polymers [23–25], although the boundary between the two systems remains vaguely defined [26]. 2D COFs are regularly porous polymers generated from preorganized rigid planar monomers through the formation of dynamic covalent bonds such as imine, hydrazone or borate bonds. However, its rigidity and insolubility categorize it as a separate family of porous solid-state materials. For many years, 2D polymers with internal pores had been 'just a dream of synthetic chemists' due to the synthetic challenge [27]. Photo-induced polymerization of monomers in crystals, followed by exfoliation of monolayers, afforded the first example of 2D polymers. Later, direct formation of soluble monolayer 2D polymers with predictable pore size has also been reported using different synthetic approaches [23]. However, the function of such structurally amazing polymers remains to be addressed. Stacking of 2D COFs or polymers can give rise to 3D structures. Actually, as there have been only limited success in exfoliating 2D COFs into monolayers, all reported 2D COFs, as well as the above-mentioned photo-initiated polymerized crystals, may be treated as 'supramolecular' 3D architectures considering the non-covalent nature between the stacked 2D layers. There are many reports that describe the so-called 3D polymers [28] or supramolecular networks [29]. Covalently and non-covalently bonded networks formed by flexible molecules or macromolecules may expand to accommodate discrete guests, but typically they exist in a collapsed form and lack regularity. When rigid conjugated units are used as the backbone, the resulting polymers may spontaneously form permanent pores of varying sizes or be perforated by using various chemical or physical methods. 3D COFs and organic porous polymers [30] represent a body of more ordered conjugated polymers with defined pores.

Similarly to COFs, the metal-organic frameworks (MOFs), formed by coordination of preorganized multi-armed ligands (linkers) to metal ions, are another well-known class of porous solid-state materials [31–33]. As a subclass of coordination polymers [34], typically MOFs have a higher regularity than COFs, but both materials feature porosity. As MOFs possess a higher diversity of backbones and a large number of metal nodes, they can exhibit more abundant functions or applications.

Although, in the past two decades, both MOFs and COFs have been among the hot topics of porous framework materials, chemists had started exploring the construction of porous molecular crystals dating back to the 1990s [35] and, since then, investigations of guest encapsulation by molecular cages have been continually flourishing [10–12]. More recently, it was established that molecular crystals can also give rise to porous channels capable of guest exchange [36]. Within this category, several examples of hydrogen bonded organic frameworks (HOFs) have been reported, which are able to selectively separate one gas from another [37]. Interests in the studies of porous materials mainly come from the fact that they possess large surfaces. For conventional zeolites, a large surface is probably the most important feature for their wide application in industrial catalysis. MOFs and COFs are more regular porous architectures with large surfaces and consequently sizes. The organic ligand components of MOFs also allow the incorporation of additional functional groups as well as post-modifications. Actually, in recent years, studies on the functions of MOFs have expanded to nearly all aspects of materials science [38]. Nevertheless, all the above-mentioned porous architectures display their porosity in the solid state and, in a book published in 1998, 'porous materials' has been defined as 'solids containing pores' [39].

Tremendous advances in solid-state porous materials nurtured the possibility of constructing extended, well-defined porous systems from molecular building blocks in solution. As covalently

bonded and metal-coordination-driven regular porous structures are all found to exist only in solids, self-assembly logically provides another 'soft' route for addressing this challenge. Since 2013, a variety of 2D and 3D well-defined self-assembled porous systems of this family, termed supramolecular organic frameworks (SOFs), have been constructed in water [40]. In most cases, cucurbitu[8]ril (CB[8])-promoted, hydrophobically driven dimerization of aromatic units has been used as the driving force. In several other examples, conjugated radical cation dimerization, donor–acceptor interaction and electrostatic attraction can also drive the framework formation. Conceptually, SOFs represent a special kind of supramolecular polymers that possess substantially increased structural regularity, which allows enhanced capacity of encapsulation. Although the library of SOFs is still relatively small and in need of expansion, more examples of SOFs have begun to emerge to bring about unique functions. This review summarizes advances in the construction of the new structures and their functions.

SUPRAMOLECULAR POLYMERS AND GELS

Since the first report of supramolecular polymers that are generated from linear monomers driven by non-covalent forces [41,42], this family of soft matter has received increasing attention [43,44]. The reversibility of non-covalent forces endows supramolecular polymers with many more prominent characters, including increased processability and stimuli-responsiveness, better recycling and self-healing capability, which are all potentially useful for the design of advanced smart materials [45–49]. Following the approaches for the preparation of covalent polymers, various monomers have been designed for generating supramolecular polymers with main-chain, (co)block and cross-linked backbones [43,44]. Given the flexibility of the backbones, at high enough concentrations, all supramolecular polymers are expected to generate 3D networks. The networks may be strong enough to suppress the flow of solvent molecules to give rise to discrete organo- or hydrogels [50–52]. Many supramolecular hydrogels can also entrap drugs and thus have been widely studied as drug-delivery carriers [53,54]. As for the characterization of these supramolecular networks, typically, different electron microscopic techniques are applied to investigate their morphologies after being dried [55,56]. In most cases, fibers or fibrous networks are observed, but neither of them reflects the fine structures of the solvent-contained networks in the gels. In principle, more regular or defined networks may favor enhanced and/or more selective encapsulation of guests. For many years, this possibility had not been explored systematically.

SELF-ASSEMBLY FROM FLEXIBLE MULTI-ARMED BUILDING BLOCKS

Star polymers represent a large class of branched macromolecular architectures with linear 'arms' radiating from a central branching core to produce higher-order 3D architectures [57]. From the point of self-assembly, star-shaped multi-armed monomers may undergo intermolecular binding to form similar supramolecular polymers [58,59]. To improve the regularity of the supramolecular networks, two straightforward approaches can be proposed: shortening the length of the branched arms and/or increasing the rigidity of the arms. It can be expected that preorganized multi-armed monomers should exhibit considerable multivalency [60,61], leading to increased stability and ordering of the corresponding supramolecular networks. One early inspiring example reported by Richert and co-workers involved the self-assembly of compounds **1a**-**1c** (Fig. 1), whose rigid core bears four or six G·C nucleic acid chains, respectively [62]. The short G·C chain alone could not dimerize in highly competitive water, but it was found that the G·C chains of **1a**-**1c** all underwent strong intermolecular dimerization in dilute aqueous solution (10 μM) through the hydrogen bonding of G·C base pairs. The solution of **1a** and **1b** turned into turbidity at 10 and 25°C, indicating the formation of large particles. Remarkably, **1c** started precipitating at 95°C and the precipitate did not fully re-dissolve upon reheating at 95°C, displaying the highest multivalence.

Hydrophobicity-driven encapsulation of cucurbitu[8]ril (CB[8]) for aromatic dimers is the most useful binding motif for the formation of supramolecular networks from multi-armed building blocks [63–65]. In this category, Zhang and co-workers demonstrated that the appended naphthalene (NP) units of tri- and four-armed compounds **2** and **3** (Fig. 1) underwent intermolecular dimerization that was remarkably enhanced through the encapsulation by CB[8] [66,67]. Both mixtures produced stable supramolecular polymers in water and, for **3**, the supramolecular polymeric structures inhibited the aggregation of its porphyrin unit, leading to enhancement of its efficiency in generating $^1O_2$. The backbone of compound **3** is quite rigid. Thus, the supramolecular polymer formed by **3** and CB[8] should possess well-defined pores, even though this character was not explored.

Due to the existence of the methylene units, the appended NP units of **2** and **3** have the freedom

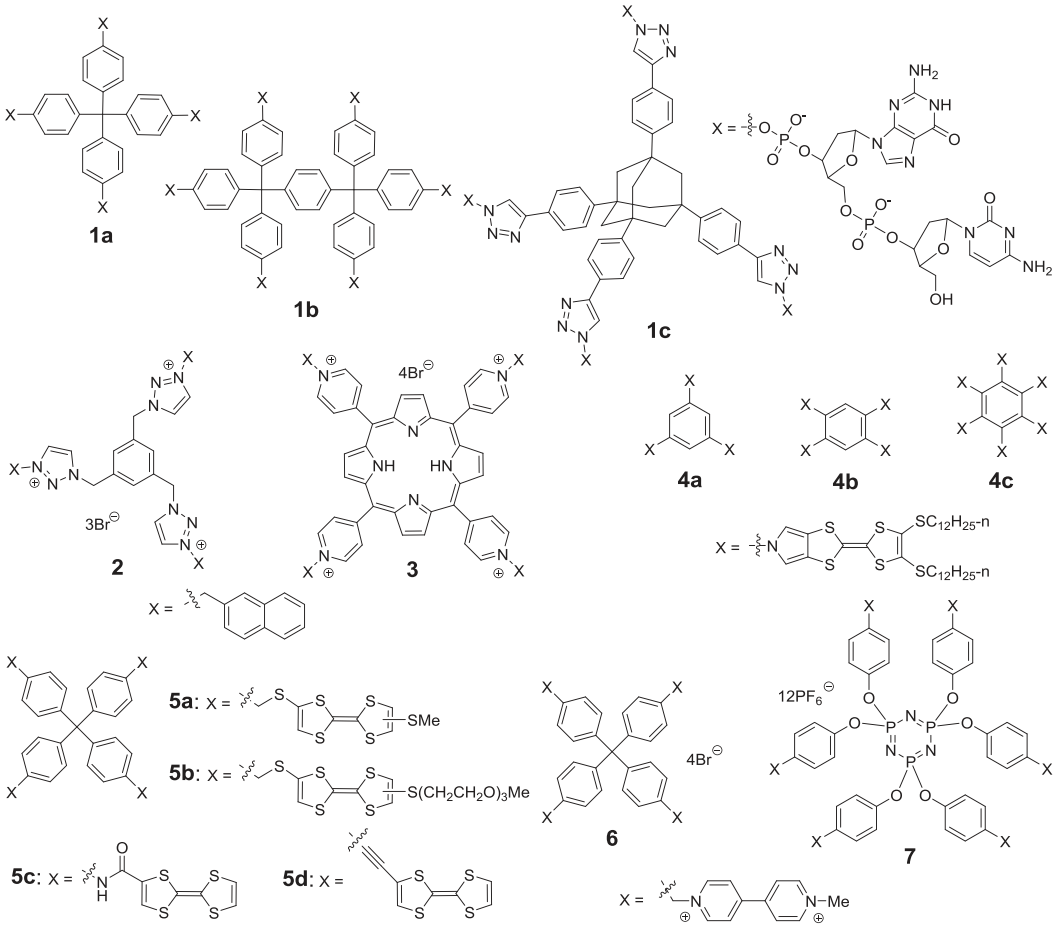

Figure 1. The structures of compounds **1**–**7**.

to rotate. Therefore, neither molecules stacks selectively in the 1D or 2D space. Fully rigid conjugated molecules tend to stack in the 1D space, which maximizes the face-to-face contact of two molecules and incurs cooperativity between different stacking units. For example, Iyoda and co-workers reported that, when the peripheral tetrathiafulvalene (TTF) units of planar **4a-c** (Fig. 1) were oxidized to $TTF^{\bullet+}$ in dichloromethane and acetonitrile (2:1 v/v), the molecules aggregated in the 1D space to give rise to long fibrils [68]. The driving force mainly came from the face-to-face stacking of the $TTF^{\bullet+}$ units [69]. We prepared tetrahedral compounds **5a-d** (Fig. 1), which bear four TTF units connected with different linkers [70,71]. The TTF units in all four compounds can be readily oxidized by $Fe(ClO_4)_3$ to $TTF^{\bullet+}$. In organic solvents, such as dichloromethane and chloroform, and water (for **5b**), their $TTF^{\blacksquare+}$ units underwent strong intermolecular stacking to generate 3D supramolecular polymers. Notably, the backbones of **5c** and **5d** were more rigid than these of **5a** and **5b**, but their $TTF^{\blacksquare+}$ dimerization in chloroform was weaker, implying that intermolecular $TTF^{\blacksquare+}$ stacking of the two more rigid molecules might produce tension due to conformational torsion. We further prepared tetrahedral **6** and reduced its four bipyridinium (BIPY) units to radical cation $BIPY^{\blacksquare+}$ in water with sodium dithionate [72]. The $BIPY^{\blacksquare+}$ units also stacked strongly in water to produce supramolecular polymers that should be structurally similar to those formed by **5a-d**. Trabolsi and co-workers prepared phosphazene derivative **7**, which contains six BIPY units, and reduced them to $BIPY^{\blacksquare+}$ [73]. It was found that these $BIPY^{\blacksquare+}$ units exclusively underwent intramolecular stacking. Clearly, for 'crowded' molecules bearing multiple binding arms, rational design of rigid backbones as well as linkers is necessary for selective intermolecular binding.

The self-assembly of compounds **1**–**6** into different supramolecular polymeric networks effectively demonstrates the efficiency of multi-armed monomers in generating multivalency and cooperativity, which can remarkably enhance inherently weak intermolecular bindings. The possibility of generating regular pores by supramolecular polymers

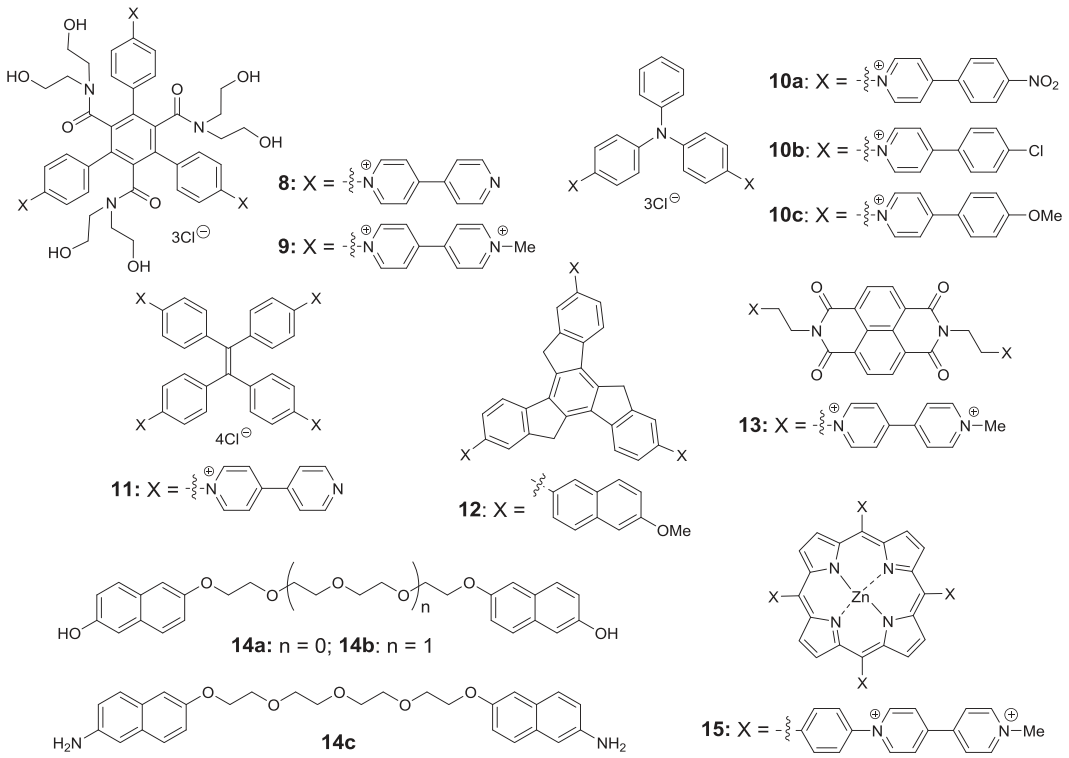

Figure 2. The structures of compounds **8**–**15**.

formed by **5a-d** and **6** in solution has been investigated. No evidence was found to support the formation of regular frameworks by all these systems. These results suggest that, for the generation of regular networks, despite the high stability incurred from supramolecular polymerization, the motion of molecular building blocks, such as backbone vibration and group swinging and rotation, has to be suppressed considerably. Our and other groups' research showed that, for the formation of 2D regular pores, the 1D stacking of planar building blocks also has to be inhibited.

2D SOFs

The formation of SOFs is mainly based on two important concepts: preorganization and multivalence, both of which are expected to enable stable binding and ordering of the resulting supramolecular architectures. The first homogeneous 2D SOF was reported in 2013 [74]. For the formation of periodic pores in the 2D space, we prepared compound **8**, which has a fully rigid triangular backbone (Fig. 2). The three cationic *N*-phenyl-4,4′-bipyridinium (PBP) units and the three hydrophilic side chains provided good solubility in water. The three glycol chains also forced the three neighboring benzene rings to twist nearly perpendicularly from the central benzene ring, which efficiently suppressed any face-to-face stacking. ^{1}H NMR and dynamic light-scattering (DLS) experiments in water supported that **8** and CB[8] (2:3) formed stable supramolecular entities. DLS experiments gave an average hydrodynamic diameter (D_H) of 69 nm at [**8**] = 2.1 mM. The value increased to about 200 nm at [**8**] = 5.2 mM. Upon evaporation of the solvent, the mixture could turn into a hydrogel. Solution-phase small-angle X-ray scattering (SAXS) experiments in water revealed a scattering peak with a *d*-spacing of 3.6 nm, which was consistent with the pore diameter (3.7 nm) calculated for a honeycomb supramolecular framework (SOF) formed from **8** and CB[8] through the encapsulation of the PBP dimer by CB[8] (Fig. 3). Powder X-ray diffraction (PXRD) experiments for the solid sample revealed a broad (100) peak with a *d*-spacing of 3.7 nm, while synchrotron X-ray scattering profile of the solid sample showed a scattering peak with a *d*-spacing of 3.8 nm, supporting that the periodicity of this SOF was maintained in the solid state. Atom force microscopy (AFM) imaging showed planar aggregates of large sizes with a height around 1.72 nm, which matched the diameter of CB[8] (1.75 nm), supporting the monolayer nature of the 2D framework.

Trimethylation of **8** with iodomethane afforded, after ion exchange, highly water-soluble **9** in

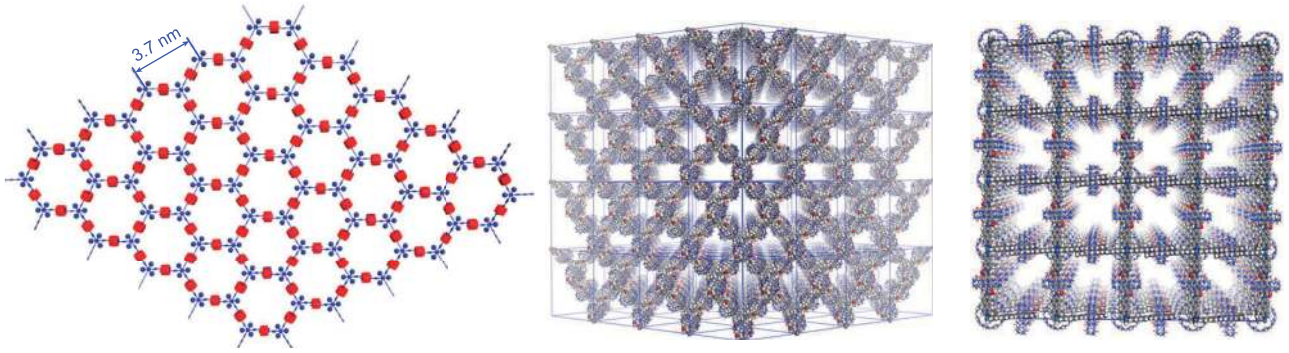

Figure 3. Modeled structures of (left) 2D honeycomb SOF formed by triangular molecule **8** and CB[8], reprinted with permission from [74]. Copyright 2014 American Chemical Society; (middle) 3D diamondoid SOF formed by tetrahedral **16** and CB[8]; and (right) 3D cubic metal ion-cored SOF formed by octahedral **17** and CB[8].

quantitative yield [75]. After the $BIPY^{2+}$ units of **9** were reduced with sodium dithionate to $BIPY^{\bullet+}$, the molecule could also form 2D SOF through the intermolecular dimerization of the $BIPY^{\bullet+}$ units [69]. CB[8] further stabilized the SOF by encapsulating the $(BIPY^{\bullet+})_2$ units.

Zhao and co-workers prepared triphenylamine (TPA) derivatives **10a-c** [76,77]. It was revealed that the 2:3 mixtures of **10a** and **10b** with CB[8] can form highly thermally stable hydrogels by forming monolayer 2D supramolecular polymers, which did not undergo phase change even at 175°C in a sealed tube. Although TPA has a cone-shaped conformation, the SAXS profile of the hydrogels still exhibited two scattering peaks corresponding to *d*-spacings of 3.6 nm (100) and 1.8 nm (200), supporting the periodicity of the 2D honeycomb structures. The 2:3 mixture of **10c** and CB[8] also formed similar 2D SOF in water [77]. Zhao and co-workers further prepared tetraphenylethene (TPE) derivative **11** (Fig. 3) and found that its 1:2 mixture with CB[8] in water formed a 2D SOF with unique parallelogram pores [78].

Feng and co-workers reported that CB[8] encapsulation-enhanced donor–acceptor interaction between the electron-rich NP units of **12** and the electron-deficient BIPY units of **13** could drive the three components to form another 2D SOF in water [79]. This framework has been transferred to surface as monolayers with a thickness of 1.8 nm, homogeneously covering areas up to 0.25 cm^2. The film was also found to be free-standing over holes of 10 μm^2. This CB[8] encapsulation-enhanced donor–acceptor interaction has also been utilized for constructing other 2D SOFs. For example, Zhao and co-authors prepared NP-derived linear monomers **14a** and **14b** and porphyrin-based square monomer **15** [80]. The intermolecular NP/$BIPY^{2+}$ donor–acceptor interaction alone was very weak, but was remarkably enhanced by CB[8]. Solution-phase SAXS profiling in water revealed a broad, but clear, scattering peak for both mixtures, corresponding to the *d*-spacing centered at 5.5 and 7.7 nm, even though both **14a** and **14b** contain a flexible linker. We found that 2D honeycomb SOFs were formed from the mixture solutions of **14b** and **14c** with **9**, as was confirmed by solution-phase SAXS experiments from which a spacing of 7.7 nm was revealed for both systems [81].

3D SOFs

The success of utilizing CB[8]-encapsulation-enhanced aromatic dimerization as the driving force for constructing 2D SOFs prompted us to prepare tetrahedral molecule **16** [82] and octahedral $[Ru(BPY)_3]^{2+}$ **17** (Fig. 4) [83]. A study on model molecule 4-(4-methoxyphenyl)-*N*-methylpyridinium revealed that its dimerization in water was substantially promoted by CB[8] through encapsulation. This three-component host–guest motif has been used for constructing a 2D SOF [77]. The methylene units endowed the backbone with certain flexibility, because a fully rigid backbone lacking this methylene unit was found to interact with CB[8] too strongly such that they formed insoluble solids.

As expected, the 1:2 mixture of **16** and CB[8] in water did form 3D diamondoid SOF. At [**16**] = 1.5 mM, DLS showed that the SOF had a D_H of 91 nm, which increased to 100 nm at [**16**] = 2 mM. The solution was found to turn into hydrogel upon evaporation of water. This 3D SOF adopted a diamondoid topology. Simulation of such a network (Fig. 3, middle) revealed periodic porous aperture of 2.1 nm, as defined by the six CB[8] units in one self-assembled macrocycle that adopts a cyclohexane-like chair conformation. SAXS experiments in water revealed a broad peak, corresponding to a *d*-spacing of around 5.1 nm,

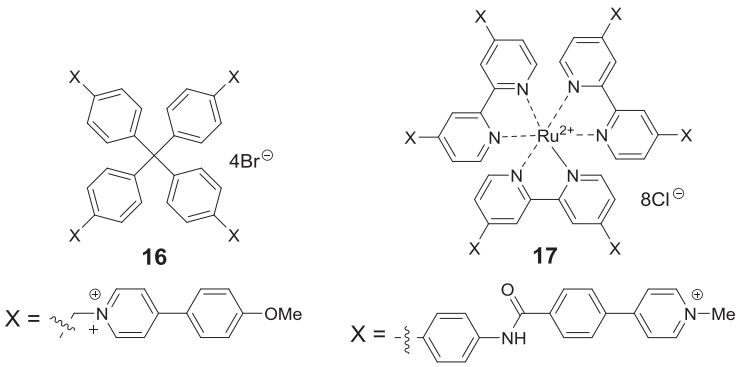

Figure 4. The structures of compounds **16** and **17**.

which matched with the calculated {100} spacing (4.9 nm) of the modeled network. Synchrotron radiation X-ray scattering reproduced this scattering peak but as a much stronger one, together with another peak assignable to the {200} spacing (2.5 nm). Synchrotron X-ray diffraction (XRD) profiling of the same solution exhibited peaks around 1.7 and 1.0 nm, which matched with the expected {220} spacing (1.7 nm) and {422} spacing (1.0 nm). The aqueous solution of this 3D SOF could turn into a hydrogel after slow evaporation, which would slowly solidify to afford microcrystals upon further evaporation. The XRD profile of the microcrystals exhibited three peaks at 5.0, 1.7 and 1.0 nm, which matched the {100}, {220} and {422} spacings, respectively, while the synchrotron SAXS profile displayed a much stronger peak centered at 4.9 nm, consistently with the {100} spacing. 2D synchrotron X-ray scattering could reveal two peaks (2.5 and 1.7 nm), matching the {200} and {220} spacings, respectively. High-resolution transmission electron microscopy (TEM) imaging could resolve the periodic porosity with 1.7 nm spacing, more directly pointing to the {220} face. All these observations supported that the 3D SOF maintained its periodicity in the solid state.

To construct cubic SOF, preorganized octahedral building blocks have to be designed. We chose to use the stable $[Ru(bpy)_3]^{2+}$ complex as the core to prepare such monomers. To increase the rigidity of the molecule, we used amide as the linker to introduce six *N*-methyl-4-phenylpyridinium units. The resulting octacationic complex **17** exhibited modest solubility in water. Its 1:3 mixture with CB[8] gave rise to the first supramolecular metal-organic framework (SMOF) in water. Synchrotron SAXS profile at [**17**] = 3.0 mM exhibited a strong peak related to the *d*-spacing around 3.1 nm, which matched with the {100} spacing (3.0 nm) of the modeled network. This peak could be observed even at a low concentration of 0.6 mM (**17**). The synchrotron XRD profile of the same solution displayed two peaks at around 3.0 nm and 2.1 nm, which can be assigned to the spacing of the {100} and {110} (2.1 nm) faces. Upon evaporation, the solution of SMOF slowly solidified and finally formed microcrystals. The XRD profile of the microcrystals exhibited three peaks at 3.0, 2.1 and 1.7 nm, matching the {100}, {110} and {111} (1.7 nm) spacings of the modeled 3D framework. The SAXS profile displayed a sharp peak at 3.0 nm relating to the {100} spacing. These results supported that the periodicity of SMOF could also be maintained in solid. On the basis of the modeled structure, the void volume of cubic SMOF was estimated to be 80% and the pore aperture, defined by the four CB[8] units in one self-assembled macrocycle adopting a square-like conformation, was calculated to be about 1.5 nm.

FUNCTIONS OF 2D AND 3D SOFs

The exploration of the functions of homogeneous SOFs is still at the early stage. Nevertheless, a number of SOFs already exhibit unique properties and functions. For example, Zhao and co-workers found that the formation of SOFs remarkably reduced the motion of molecular building blocks and the rotation and vibration of subunits. For 2D SOF formed by **10c** and CB[8], the fluorescence of **10c** in the framework was enhanced by 35 times compared to that of **10c** [76]. The low emissive property of **10c** was attributed to intramolecular charge transfer between the electron-rich TPA unit and the connected electron-deficient pyridinium unit. This process was blocked by the encapsulation of the pyridinium unit by CB[8] and hence restored the emission of TPA. This 2D SOF was also revealed to be an efficient fluorescent chemosensor for the detection of picric acid with high selectivity and sensitivity, which was attributed to the donor–acceptor interaction between TPA and picric acid. Tetracationic **11** alone was nonemissive in water. Upon formation of 2D SOF with CB[8], **11** exhibited strong fluorescence, which has been attributed to CB[8]-encapsulation-induced inhibition of the rotation of the TPE core—a mechanism for aggregation-induced emission that is observed in a large number of TPE derivatives [84].

2D SOFs formed by CB[8], **9** and **14b** or **14c** have a flexible framework. As monolayer cationic supramolecular polyelectrolytes, these two SOFs were found to exhibit modest antimicrobial activity against methicillin-resistant *Staphylococcus aureus* (MRSA) in a dose-dependent manner [81], while the individual components at the identical concentration did not show any detectable activity. The activity exhibited by the two SOFs has been tentatively

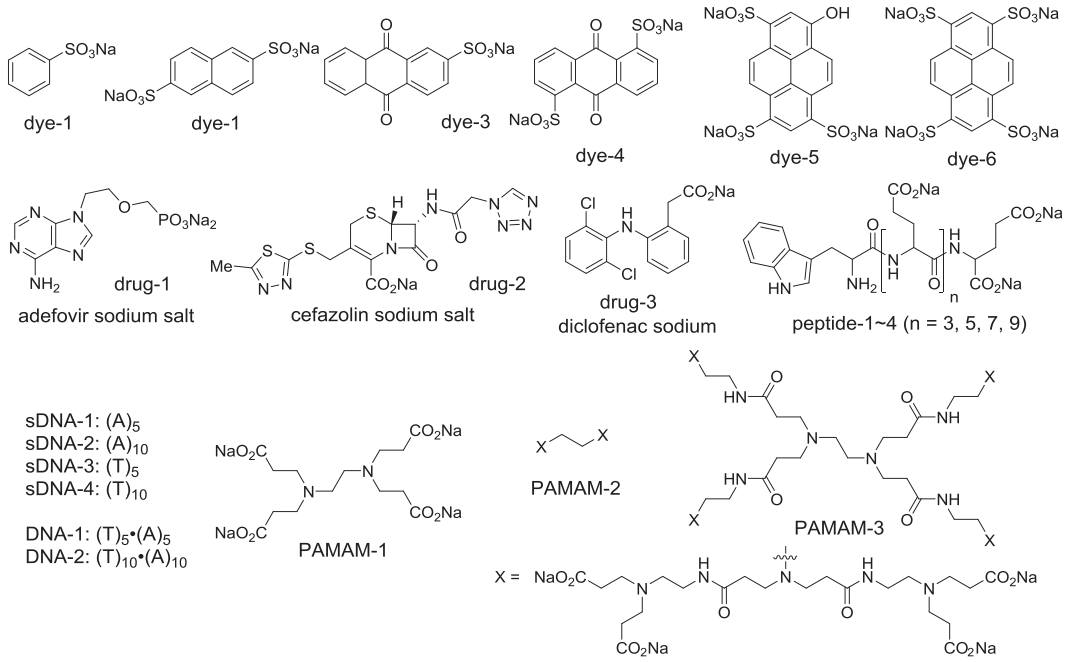

Figure 5. The structure of dye-1-6, drug-1-3, peptide-1-4, sDNA-1-4, DNA-1,2 and PAMAM-1-3.

attributed to their increased cation concentration in the 2D space on the surface of MRSA.

The capacity of 3D diamondoid and cubic SOFs for the adsorption of nitrogen was found to be very weak, which may be attributed to the polycationic nature of these frameworks. The void volume of the above diamondoid 3D SOF formed by **16** and CB[8] was estimated to be 77% [82]. As a 3D supramolecular polyelectrolyte with regular porosity, this SOF exhibited extremely strong capacity of adsorbing anionic organic guests, including dye 1–6, drug 1–3, peptide 1–4, sDNA-1-4, DNA-1,2 and dendrimer 1–3 (Fig. 5), which can be rationalized on the basis of 'hard and soft acids and bases' theory. Adsorption of the anionic guests, as soft bases, led to the formation of soft acid (pyridinium)-soft base ion pairs and hard acid (Na^+)-hard base (Br^-) ion pairs. Figure 6 shows the concentration-dependent fluorescence quenching of the 4-(*N*-methylpyridyl)anisole unit by the three drugs in water. As the fluorescence of control was not affected by excessive amounts of the drugs, the efficient fluorescence quenching reveals that, even at very low concentrations, the adsorption of the framework for anionic drugs is still of high efficiency, implying the potential application of the 3D SOF as homogeneous drug carriers. Diamondoid 3D SOF microcrystals formed after slow evaporation of the solvent were found to be extremely stable and insoluble in water even at 100°C. Thus, the microcrystals (1.0 mg) were found to be able to extract the anionic guests, with [anion] = [cation], from solution.

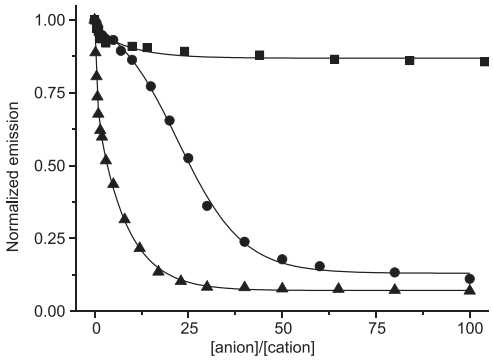

Figure 6. Fluorescence quenching of the 4-(*N*-methylpyridyl)anisole unit (0.02 mM) of diamondoid 3D SOF at 450 nm in water by drug-1-3. [anion] represents the total concentration of the anionic unit of the guests.

After 60 hours, extraction reached equilibrium except for DNA-2 and the extracting percentage of eight guests exceeded 75%, and was nearly quantitative for dye-5 and dye-6. When the guest-loaded microcrystals were immersed in a $MeCO_2H/MeCO_2Na$ buffer (pH = 4.9) on a shaking orbital shaker, most of the guests could be released to solution after 60 hours.

In water, the 3D cubic SMOF could accommodate bulky functional anionic species, such as redox-active Wells–Dawson-type polyoxoanions $[P_2W_{18}O_{62}]^{6-}$ (WD-POM) [83], which has a width of about 1.1 nm. Remarkably, this encapsulation occurred in a one-cage-one-POM manner, which meant that every $Ru(bpy)_3^{2+}$ or encapsulated

WD-POM cluster was mutually surrounded by eight counterparts at the vertices of a cubic cage. SAXS and XRD experiments supported that POM-loaded SMOF maintained its periodicity in both solution and the solid state. The one-cage-one-POM encapsulation pattern is ideal for photo-initiated electron transfer from excited $Ru(bpy)_3^{2+}$ to redox-active WD-POM [85]. Thus, visible-light (500-nm)-initiated sensitization of $[Ru(bpy)_3]^{2+}$ for the catalytic reduction of proton into hydrogen gas by WD-POM was studied in acidic aqueous solution (pH = 1.8) using methanol as the sacrificial electron donor. It was found that, at $[Ru^{2+}]$ = 0.3 mM and [POM] = 0.002 mM, the turnover number (TON), defined as $n(0.5H_2)/n$POM, for H_2 production reached 392, which corresponded to a H_2 evolving rate, i.e. turnover frequency (TOF), of 3553 μmol/g/h (based on POM). This level of H_2 production is about four times higher than that of a heterogeneous WD-POM@$[Ru(bpy)_3]^{2+}$-MOF system containing the identical amounts of WD-POM and $[Ru(bpy)_3]^{2+}$ units [85]. The high efficiency of the WD-POM@SMOF system has been attributed to its unique one-cage-one-POM arrangement and homogeneity, which allowed quick diffusion and close contact of hydronium and methanol molecules, and facilitated the electron transfer from excited $[Ru(bpy)_3]^{2+}$ to WD-POM. Heterogeneous H_2 production was also realized using WD-POM@SMOF microcrystals (molar ratio: 1:15) as catalysts in acetonitrile and DMF (3:7), in which the microcrystals were insoluble. With methanol and triethanolamine as the sacrificial electron donors, TON reached 48 and 1820 after irradiation for 14 hours. The latter value is about five times higher than that of the heterogeneous WD-POM@$[Ru(bpy)]_3^{2+}$-MOF hybrid [85].

CONCLUSION AND OUTLOOK

Generally, we may consider homogeneous periodic 2D and 3D SOFs as a family of soft porous materials that can exist in both solution and the solid state. The self-assembly conditions for the formation of these new organic porous materials are extremely mild—just dissolve the components of the required ratio in water! Such assembly has been only demonstrated in water but should not be limited to just water and could be extended to other solvents. This is in sharp contrast to the harsh solvothermal, mainly hydrothermal, conditions for the generation of MOFs and COFs. 2D SOFs are more structurally diverse and have been revealed to exhibit interesting functions in tuning the fluorescence of conjugated segments and antimicrobial activity, while the functions of 3D SOFs are closely related to their porosity to adsorb anionic guests with a remarkably high efficiency. The 3D SMOF represents the first example of soluble MOFs that are generated through non-covalent force, which allows the investigation of MOF-like functions in a homogeneous way. As a family of homogeneous water-soluble porous architectures, SOFs may also be expected to find applications as biomedical materials in the future.

The adsorption of anionic organic guests into the internal of 3D SOFs opens the door for exploiting new functions. For example, the adsorption of diamondoid SOFs for drugs may be utilized for creating new delivery systems with controlled release profiles. The one-cage-one-guest encapsulation pattern of cubic SOFs may be applied for constructing new 3D light-harvesting systems. The cages of 3D diamondoid and cubic SOFs are large enough to accommodate two or more molecules and thus may also be used to impose control on the selectivity of multi-component reactions, particularly those through dynamic covalent chemistry. We envision that all these possibilities could be addressed by modifications of the monomers and expansion of the pores of the framework.

FUNDING

We thank the Ministry of Science and Technology (2013CB834501), the Ministry of Education (Doctor Fellowship Grant), the National Natural Science Foundation of China (21432004, 21529201 and 91527301), and the Science and Technology Commission of Shanghai Municipality for financial support and beamlines BL16B1 and BL14B1 (Shanghai Synchrotron Radiation Facility) for providing the beam time and helps during experiments. Y.L. gives thanks for the support from the Molecular Foundry, Lawrence Berkeley National Laboratory, supported by the Office of Science, Office of Basic Energy Sciences, Scientific User Facilities Division, of the U.S. Department of Energy under Contract No. DE-AC02-05CH11231.

Conflict of interest statement. None declared.

REFERENCES

1. Pedersen CJ. The discovery of crown ethers. *Angew Chem Int Ed Engl* 1988; **27**: 1021–7.
2. Lehn JM. Supramolecular chemistry: molecules, supramolecules, and molecular functional units. *Angew Chem* 1988; **100**: 91–116.
3. Cram DJ. The design of molecular hosts, guests, and their complexes. *Angew Chem Int Ed Engl* 1988; **27**: 1009–20.
4. Cram DJ. Molecular container compounds. *Nature* 1992; **356**: 29–36.
5. Jin Y, Wang Q and Taynton P *et al*. Dynamic covalent chemistry approaches toward macrocycles, molecular cages, and polymers. *Acc Chem Res* 2014; **47**: 1575–86.

6. Giri N, Del Popolo MG and Melaugh G *et al.* Liquids with permanent porosity. *Nature* 2015; **527**: 216–20.
7. Zhang G and Mastalerz M. Organic cage compounds: from shape-persistency to function. *Chem Soc Rev* 2014; **43**: 1934–47.
8. Yoshizawa M and Fujita M. Self-assembled coordination cage as a molecular flask. *Pure Appl Chem* 2005; **77**: 1107–12.
9. Hof F, Craig SL and Nuckolls C *et al.* Molecular encapsulation. *Angew Chem Int Ed* 2002; **41**: 1488–508.
10. Harris K, Fujita D and Fujita M. Giant hollow MnL_{2n} spherical complexes: structure, functionalisation and applications. *Chem Commun* 2013; **49**: 6703–12.
11. Amouri H, Desmarets C and Moussa J. Confined nanospaces in metallocages: guest molecules, weakly encapsulated anions, and catalyst sequestration. *Chem Rev* 2012; **112**: 2015–41.
12. Dalgarno SJ, Atwood JL and Raston CL. Sulfonatocalixarenes: molecular capsule and 'Russian doll' arrays to structures mimicking viral geometry. *Chem Commun* 2006; 4567–74.
13. Montenegro J, Ghadiri MR and Granja JR. Ion channel models based on self-assembling cyclic peptide nanotubes. *Acc Chem Res* 2013; **46**: 2955–65.
14. Chapman R, Danial M and Koh ML *et al.* Design and properties of functional nanotubes from the self-assembly of cyclic peptide templates. *Chem Soc Rev* 2012; **41**: 6023–41.
15. Shimizu LS, Salpage SR and Korous AA. Functional materials from self-assembled bis-urea macrocycles. *Acc Chem Res* 2014; **47**: 2116–27.
16. Wei X, Zhang G and She Y *et al.* Persistent organic nanopores amenable to structural and functional tuning. *J Am Chem Soc* 2016; **138**: 2749–54.
17. Sakai N and Matile S. Synthetic ion channels. *Langmuir* 2013; **29**: 9031–40.
18. Yashima E, Ousaka N and Taura D *et al.* Supramolecular helical systems: helical assemblies of small molecules, foldamers, and polymers with chiral amplification and their functions. *Chem Rev* 2016; **116**: 13752–990.
19. Guo R, Zhang L and Wang H *et al.* Hydrophobically driven twist sense bias of hollow helical foldamers of aromatic hydrazide polymers in water. *Polym Chem* 2015; **6**: 2382–5.
20. Côté AP, Benin AI and Ockwig NW *et al.* Porous, crystalline, covalent organic frameworks. *Science* 2005; **310**: 1166–70.
21. Ding SY and Wang W. Covalent organic frameworks (COFs): from design to applications. *Chem Soc Rev* 2013; **42**: 548–68.
22. Liu XH, Guan CZ and Wang D *et al.* Graphene-like single-layered covalent organic frameworks: synthesis strategies and application prospects. *Adv Mater* 2014; **26**: 6912–20.
23. Payamyar P, King BT and Öttinger HC *et al.* Two-dimensional polymers: concepts and perspectives. *Chem Commun* 2016; **52**: 18–34.
24. Zhou TY, Lin F and Li ZT *et al.* Single-step solution-phase synthesis of freestanding two-dimensional polymers and their evolution into hollow spheres. *Macromolecules* 2013; **46**: 7745—52.
25. Rodríguez-San-Miguel D, Amo-Ochoaa P and Zamora F. MasterChem: cooking 2D-polymers. *Chem Commun* 2016; **52**: 4113–27.
26. Cai SL, Zhang WG and Zuckermann RNF. The organic flatland—recent advances in synthetic 2D organic layers. *Adv Mater* 2015; **27**: 5762–70.
27. Sakamoto J, van Heijst J and Lukin OF. Two-dimensional polymers: just a dream of synthetic chemists? *Angew Chem Int Ed* 2009; **48**: 1030–69.
28. Flory PJ. Molecular size distribution in three-dimensional polymers. I. Gelation. *J Am Chem Soc* 1941; **63**: 3083–90.
29. Yount WC, Loveless DM and Craig SL. Strong means slow: dynamic contributions to the bulk mechanical properties of supramolecular networks. *Angew Chem Int Ed* 2005; **44**: 2746–8.
30. Trewin A and Cooper AI. Porous organic polymers: distinction from disorder? *Angew Chem Int Ed* 2010; **49**: 1533–5.
31. Rowsell JLC and Yaghi OM. Metal-organic frameworks: a new class of porous materials. *Microporous Mesoporous Mater* 2004; **73**: 3–14.
32. Xuan W, Zhu C and Liu Y *et al.* Mesoporous metal-organic framework materials. *Chem Soc Rev* 2012; **41**: 1677–95.
33. Zhang CW, Chen LJ and Yang HB. Pillarene-involved metallic supramolecular nanostructures. *Chin J Chem* 2015; **33**: 319–28.
34. Swiegers GF and Malefetse TJ. New self-assembled structural motifs in coordination chemistry. *Chem Rev* 2000; **100**: 3483–537.
35. Hashim MI, Hsu CW and Le HTM *et al.* Organic molecules with porous crystal structures. *Synlett* 2016; **27**: 1907–18.
36. Kawano M and Fujita M. Direct observation of crystalline-state guest exchange in coordination networks. *Coord Chem Rev* 2007; **251**: 2592–605.
37. He Y, Xiang S and Chen B. A microporous hydrogen-bonded organic framework for highly selective C_2H_2/C_2H_4 separation at ambient temperature. *J Am Chem Soc* 2011; **133**: 14570–3.
38. Furukawa H, Cordova KE and O'Keeffe M *et al.* The chemistry and applications of metal-organic frameworks. *Science* 2013; **341**: 974.
39. Ishizaki K, Komarneni S and Nanko M (eds). *Porous Materials*. Dordrecht: Kluwer, 1998.
40. Tian J, Chen L and Zhang DW *et al.* Supramolecular organic frameworks: engineering periodicity in water through host—guest chemistry. *Chem Commun* 2016; **52**: 6351–62.
41. Fouquey C, Lehn JM and Levelut AM. Molecular recognition directed self-assembly of supramolecular liquid crystalline polymers from complementary chiral components. *Adv Mater* 1990; **2**: 254–7.
42. Dong S, Zheng B and Wang F *et al.* Supramolecular polymers constructed from macrocycle-based host–guest molecular recognition motifs. *Acc Chem Res* 2014; **47**: 1982–94.
43. Brunsveld L, Folmer BJB and Meijer EW *et al.* Supramolecular polymers. *Chem Rev* 2001; **101**: 4071–97.
44. Yang L, Tan X and Wang Z *et al.* Supramolecular polymers: historical development, preparation, characterization, and functions. *Chem Rev* 2015; **115**: 7196–239.
45. Aida T, Meijer EW and Stupp SI. Functional supramolecular polymers. *Science* 2012; **335**: 813–7.
46. Yan X, Wang F and Zheng B *et al.* Stimuli-responsive supramolecular polymeric materials. *Chem Soc Rev* 2012; **41**: 6042–65.
47. Guo DS and Liu Y. Calixarene-based supramolecular polymerization in solution. *Chem Soc Rev* 2012; **41**: 5907–21.
48. Li SL, Xiao T and Lin C *et al.* Advanced supramolecular polymers constructed by orthogonal self-assembly. *Chem Soc Rev* 2012; **41**: 5950–68.
49. Ma X and Tian H. Stimuli-responsive supramolecular polymers in aqueous solution. *Acc Chem Res* 2014; **47**: 1971–81.
50. Appel EA, del Barrio J and Loh XJ *et al.* Supramolecular polymeric hydrogels. *Chem Soc Rev* 2012; **41**: 6195–214.
51. Du X, Zhou J and Shi J *et al.* Supramolecular hydrogelators and hydrogels: from soft matter to molecular biomaterials. *Chem Rev* 2015; **115**: 13165–307.
52. Dong Y, Yang Z and Liu D. DNA nanotechnology based on i-motif structures. *Acc Chem Res* 2014; **47**: 1853–60.
53. Yang Z, Liang G and Xu B. Enzymatic hydrogelation of small molecules. *Acc Chem Res* 2008; **41**: 315–26.

54. Xiao X, Hu J and Wang X *et al.* A dual-functional supramolecular hydrogel based on a spiropyran-galactose conjugate for target-mediated and light-controlled delivery of microRNA into cells. *Chem Commun* 2016; **52**: 12517–20.
55. Yu G, Yan X and Han C *et al.* Characterization of supramolecular gels. *Chem Soc Rev* 2013; **42**: 6697–722.
56. Liu Y, Wang Z and Zhang X. Characterization of supramolecular polymers. *Chem Soc Rev* 2012; **41**: 5922–32.
57. Ren JM, McKenzie TG and Fu Q *et al.* Star polymers. *Chem Rev* 2016; **116**: 6743–836.
58. Zhang Q, Qu DH and Ma X *et al.* Sol–gel conversion based on photoswitching between noncovalently and covalently linked netlike supramolecular polymers. *Chem Commun* 2013; **49**: 9800–2.
59. Li C, Han K and Li J *et al.* Supramolecular polymers based on efficient pillar[5]arene—neutral guest motifs. *Chem Eur J* 2013; **19**: 11892–7.
60. Mulder A, Huskens J and Reinhoudt DN. Multivalency in supramolecular chemistry and nanofabrication. *Org Biomol Chem* 2004; **2**: 3409–24.
61. Xu JF, Chen L and Zhang X. How to make weak noncovalent interactions stronger. *Chem Eur J* 2015; **21**: 11938–46.
62. Singh A, Tolev M and Meng M *et al.* Branched DNA that forms a solid at 95°C. *Angew Chem Int Ed* 2011; **50**: 3227–31.
63. Ko YH, Kim E and Hwang I *et al.* Supramolecular assemblies built with host-stabilized charge-transfer interactions. *Chem Commun* 2007; 1305–15.
64. Zhang ZJ, Zhang YM and Liu Y. Controlled molecular self-assembly behaviors between cucurbituril and bispyridinium derivatives. *J Org Chem* 2011; **76**: 4682–5.
65. Zhang Y, Zhou TY and Zhang KD *et al.* Encapsulation enhanced dimerization of a series of 4-aryl-*N*-methylpyridinium derivatives in water: new building blocks for self-assembly in aqueous media. *Chem Asian J* 2014; **9**: 1530–4.
66. Fang R, Liu Y and Wang Z *et al.* Water-soluble supramolecular hyperbranched polymers based on host—enhanced π–π interaction. *Polym Chem* 2013; **4**: 900–3.
67. Liu Y, Huang Z and Liu K *et al.* Porphyrin-containing hyperbranched supramolecular polymers: enhancing $^1O_2$-generation efficiency by supramolecular polymerization. *Polym Chem* 2014; **5**: 53–6.
68. Takase M, Yoshida N and Nishinaga T *et al.* Star-shaped pyrrole-fused tetrathiafulvalene oligomers: synthesis and redox, self-assembling, and conductive properties. *Org Lett* 2011; **13**: 3896–9.
69. Zhang DW, Tian J and Chen L *et al.* Dimerization of conjugated radical cations: an emerging non-covalent interaction for self-assembly. *Chem Asian J* 2015; **10**: 56–68.
70. Tian J, Ding YD and Zhou TY *et al.* Self-assembly of three-dimensional supramolecular polymers through cooperative tetrathiafulvalene radical cation dimerization. *Chem Eur J* 2014; **20**: 575–84.
71. Chen L, Zhang SC and Wang H *et al.* Three-dimensional supramolecular polymers driven by rigid tetrahedral building blocks through tetrathiafulvalene radical cation dimerization. *Tetrahedron* 2014; **70**: 4778–83.
72. Zhou C, Tian J and Wang J-L *et al.* A three-dimensional cross-linking supramolecular polymer stabilized by the cooperative dimerization of the viologen radical cation. *Polym Chem* 2014; **5**: 341–5.
73. Wadhwa K, Nuryyeva S and Fahrenbach AC *et al.* Intramolecular redox-induced dimerization in a viologen dendrimer. *J Mater Chem C* 2013; **1**: 2302–7.
74. Zhang KD, Tian J and Hanifi D *et al.* Toward a single-layer two-dimensional honeycomb supramolecular organic framework in water. *J Am Chem Soc* 2013; **135**: 17913—8.
75. Zhang L, Zhou TY and Tian J *et al.* A two-dimensional single-layer supramolecular organic framework that is driven by viologen radical cation dimerization and further promoted by cucurbit[8]uril. *Polym Chem* 2014; **5**: 4715–21.
76. Zhou TY, Qi QY and Zhao QL *et al.* Highly thermally stable hydrogels derived from monolayered two-dimensional supramolecular polymers. *Polym Chem* 2015; **6**: 3018–23.
77. Zhang Y, Zhan T-G and Zhou T-Y *et al.* Fluorescence enhancement through the formation of a single-layer two-dimensional supramolecular organic framework and its application in highly selective recognition of picric acid. *Chem Commun* 2016; **52**: 7588–91.
78. Xu SQ, Zhang X and Nie CB *et al.* The construction of a two-dimensional supramolecular organic framework with parallelogram pores and stepwise fluorescence enhancement. *Chem Commun* 2015; **51**: 16417–20.
79. Pfeffermann M, Dong R and Graf R *et al.* Free-standing monolayer two-dimensional supramolecular organic framework with good internal order. *J Am Chem Soc* 2015; **137**: 14525—32.
80. Zhang X, Nie CB and Zhou TY *et al.* The construction of single-layer two-dimensional supramolecular organic frameworks in water through the self-assembly of rigid vertexes and flexible edges. *Polym Chem* 2015; **6**: 1923–7.
81. Zhang L, Jia Y and Wang H *et al.* PH-responsive single-layer honeycomb supramolecular organic frameworks that exhibit antimicrobial activity. *Polym Chem* 2016; **7**: 1861–5.
82. Tian J, Zhou TY and Zhang SC *et al.* Three-dimensional periodic supramolecular organic framework ion sponge in water and microcrystals. *Nat Commun* 2014; **5**: 5574.
83. Tian J, Xu ZY and Zhang DW *et al.* Supramolecular metal-organic frameworks that display high homogeneous and heterogeneous photocatalytic activity for H_2 production. *Nat Commun* 2016; **7**: 11580.
84. Hong Y, Lam JWY and Tang BZ. Aggregation-induced emission. *Chem Soc Rev* 2011; **40**: 5361–88.
85. Zhang ZM, Zhang T and Wang C *et al.* Photosensitizing metal-organic framework enabling visible-light-driven proton reduction by a Wells-Dawson-type polyoxometalate. *J Am Chem Soc* 2015; **137**: 3197–200.